

Studies on Photoinduced H-Atom and Electron Transfer Reactions of *o*-Naphthoquinones by Laser Flash Photolysis

Yang Pan,[†] Yao Fu,[‡] Shaoxiong Liu,[†] Haizhu Yu,[‡] Yuhe Gao,[§] Qingxiang Guo,[‡] and Shuqin Yu^{*,†}

Department of Chemical Physics, Department of Chemistry, and Hefei National Laboratory for Physical Sciences at Microscale, University of Science and Technology of China, Hefei 230026, China

Received: September 19, 2005; In Final Form: April 19, 2006

The quenching of the triplets of 1,2-naphthoquinone (NQ) and 1,2-naphthoquinone-4-sulfonic acid sodium salt (NQS) by various electron and H-atom donors was investigated by laser flash photolysis measurement in acetonitrile and benzene. The results showed that the reactivities and configurations of $^3\text{NQ}^*$ ($^3\text{NQS}^*$) are governed by solvent polarity. All the quenching rate constants (k_q) measured in benzene are larger than those in acetonitrile. The SO_3Na substituent at the C-4 position of NQS makes $^3\text{NQS}^*$ more reactive than $^3\text{NQ}^*$ in electron/H-atom transfer reactions. Large differences of k_q values were discovered in H-atom transfer reactions for alcohols and phenols, which can be explained by different H-abstraction mechanisms. Detection of radical cations of amines/anilines in time-resolved transient absorption spectra confirms an electron transfer mechanism. Triplets are identified as precursors of formed radical anions of NQ and NQS in photoinduced reactions. The dependence of electron transfer rate constants on the free energy changes (ΔG) was treated by using the Rehm–Weller equation. For the four anilines with different substituents on the para or meta position of amidocyanogen, good correlation between $\log k_q$ values with Hammett σ constants testifies the correctness of empirical Hammett equation. Charge density distributions, adiabatic ionization/affinity potentials and redox potentials of NQ (NQS) and some quenchers were studied by quantum chemistry calculation.

Introduction

Photochemistry of quinones has been extensively investigated because of its importance in biological systems and in photosynthesis.^{1–5} Much research has been carried out by means of laser flash photolysis,^{6,7} pulse photolysis,⁸ molecular fluorescence,⁹ time-resolved resonance Raman,¹⁰ theoretical calculation¹¹ and chemically induced dynamic electron polarization.¹²

The chemically active triplet states of quinones were expected to participate in all corresponding photochemical reactions.^{1–8} Many researchers have systematically studied the interactions of inorganic/organic compounds with the triplet states of benzoquinone, naphthoquinone, anthraquinone and their derivatives, and the electron transfer pathway was deemed to be the crucial step in various reactions.^{13,14} Sometimes a triplet exciplex with weak charge transfer character was also thought to be an important transient species.¹⁵ Small negative reduction potentials make quinones act as good electron acceptors. With carbonyl groups, H-atom abstraction from hydrogen donors would be anticipated for triplets of quinones, and relative works have been studied by a number of groups.^{16,17} The properties of H-atom/electron abstraction for quinones vary significantly due to different conformations of excited states; i.e., some quinones have $^3(\text{n},\pi)^*$ configurations that are in favor of H-atom abstraction, whereas others have $^3(\pi,\pi)^*$ conformations that are propitious for getting an electron.^{16b}

Although research concerning quinones is plentiful, there are very few papers related to *o*-quinones compared with *p*-quinones

(*p*-benzoquinone, 1,4-naphthoquinone, 9,10-anthraquinone and their derivatives). Actually, *o*-quinones such as 9,10-phenanthrenequinone (PQ) and 1,2-naphthoquinone (NQ) have some peculiarities. The energy of the T_1 state for PQ (49.1–50.0 kcal/mol) has been obtained through phosphorescence measurements.¹⁸ A lower E_T value for NQ has been obtained through theoretical calculation because of its nonphosphorescent character.^{8a,19} Due to two adjacent carbonyl groups, *o*-quinones have remarkably higher reactivities toward H-atom abstraction even than acetone and/or benzophenone with high triplet energy.¹⁸ Furthermore, TR-ESR has confirmed a dominant $^3(\pi,\pi)^*$ T_1 state of NQ in polar solvents and a $^3(\text{n},\pi)^*$ T_1 state in nonpolar solvents and has found a small energy gap between $^3(\text{n},\pi)^*$ and $^3(\pi,\pi)^*$ states.²⁰ Although the $^3(\pi,\pi)^*$ configuration is inactive toward H-atom abstraction, low lying $^3(\text{n},\pi)^*$ is deemed to be involved in such reactions with suitable H-atom donors. Solvent polarity dependence of some *o*-quinones has been investigated and indicated the reactivities of *o*-quinone triplets toward H-atom abstraction increase as the polarity of the solvent decreases.²¹ Like *p*-quinones, triplet *o*-quinones are good electron acceptors in photoinduced electron transfer reactions.¹⁷

To the best of our knowledge, only a few papers have been reported on the photoinduced H-atom and electron transfer reactions of NQ,^{17,19,21} and corresponding thermodynamic results have never been obtained. This paper presents laser flash photolysis studies on NQ and NQS with diverse electron and H-atom donors to determine the mechanisms of observed photoinduced reactions. Absorption bands of 3,5,*N,N*-tetramethylaniline and dimethyl-*p*-toluidine radical cations were detected for the first time. Quantum chemistry calculation was utilized to get useful information such as charge density

* Corresponding author. Tel.: +86 5513601119. Fax: +86 5513607084. E-mail address: sqyu@ustc.edu.cn.

[†] Department of Chemical Physics.

[‡] Department of Chemistry.

[§] Hefei National Laboratory for Physical Sciences at Microscale.

distributions and redox potentials of some molecules. E_{ox} values for the anilines from quantum calculations are found to correlate well with the Hammett σ constants. This correlation indicates the pertinence of theoretical and empirical results of different research fields. In addition, free energy changes were calculated by using the Rehm–Weller equation.

Experimental and Computational Methods

1,2-Naphthoquinone (NQ), 1,2-naphthoquinone-4-sulfonic acid sodium salt (NQS), 4-(dimethylamino)benzoic acid (DMA-BA) and diphenylamine (DPA) were obtained from Aldrich. 3,5,*N*-Tetramethylaniline (TMA), triphenylamine (TPA) and dimethyl-*p*-toluidine (DMT) were obtained from Fluka. All the foregoing reagents were used without further purification. 1,4-Diazobicyclo[2.2.2]octane (DABCO) and phenol were recrystallized from ethanol twice. 1,3-Dihydroxybenzene and 1,4-dihydroxybenzene were recrystallized from toluene twice. Triethylamine (TEA), 2-propanol, ethanol and *N,N*-dimethylaniline (DMA) were distilled twice before use. Benzyl alcohol, *sec*-butanol and phenethyl alcohol were used directly without further purification. Acetonitrile (MeCN), cyclohexane and benzene were spectrophotometric grade. The resulting solutions were bubbled with high-purity argon (99.99%) for 20 min before the spectroscopic measurements. All the spectra were recorded at ambient temperature.

The third harmonic (355 nm) of a Q-switched Nd:YAG laser (Spectra Physics, GCR-170, repetition rate of 10 Hz) with a duration of 8 ns was used as the excitation source in laser flash photolysis experiments as described previously.^{22,23}

The gas-phase geometry was optimized using density functional theory (DFT) at the B3LYP/6-31+(d) level of theory. Frequency calculations at the same level were also conducted on all the optimized structures, which confirmed that they were real minima without any imaginary frequencies. Single-point energy calculations were performed with the resulting geometries at the B3LYP/6-311++G(2df,2p) level. The PCM solvation model was used to calculate the solvation free energies in acetonitrile at B3LYP/6-31+G(d,p) level. In this method the solute cavity was modeled by the optimized molecular shape. Both the electrostatic and nonelectrostatic contributions were included for the total solvation energies. The calculations of standard redox potentials were carried out according to the computational procedure of Fu et al.²⁴

Results

1. Transient Absorption Spectra and Self-Quenching

Study of $^3\text{NQ}^*$ and $^3\text{NQS}^*$. The irradiation of NQ in deaerated acetonitrile with 355 nm laser pulse yields the transient absorption spectra with maxima at 390 nm along with two broad absorption bands around 590 and 660 nm, as shown in Figure 1a. We attribute it to laser-produced triplets of NQ which is consistent with previous reports,^{19,25} because it could be quenched drastically by dissolved oxygen, as shown in Figure 2. The transient spectra of pure NQS in acetonitrile also show an obvious absorption peak at 390 nm accompanied by a broad band between 450 and 750 nm (Figure 1b), which are similar to that of NQ. The absorptions are assigned to the excited triplets of NQS by using the method aforementioned. Due to the poor dissolvability in acetonitrile, the absorption intensity for $^3\text{NQS}^*$ is low in nature, as compared with $^3\text{NQ}^*$.

Decay time τ for $^3\text{NQ}^*$ at a given concentration was obtained by single-exponential fitting to the decay trace. According to eq 1, the self-quenching rate constant k_{sq} and triplet lifetime τ_0 for $^3\text{NQ}^*$ are determined to be $2.82 \times 10^8 \text{ M}^{-1} \text{ s}^{-1}$ and 11.3

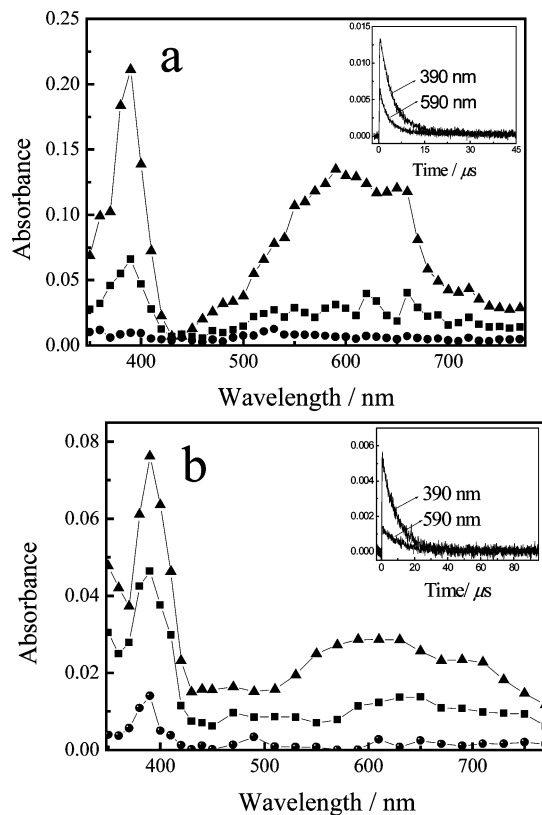


Figure 1. Transient absorption spectra observed in the laser photolysis of (a) NQ (0.35 mM) and (b) NQS (0.033 mM): 1 μs (\blacktriangle), 10 μs (\blacksquare) and 50 μs (\bullet) after 355 nm laser pulse in Ar-saturated acetonitrile. Inset: decay time profile of 390 and 590 nm bands in Ar-saturated solutions.

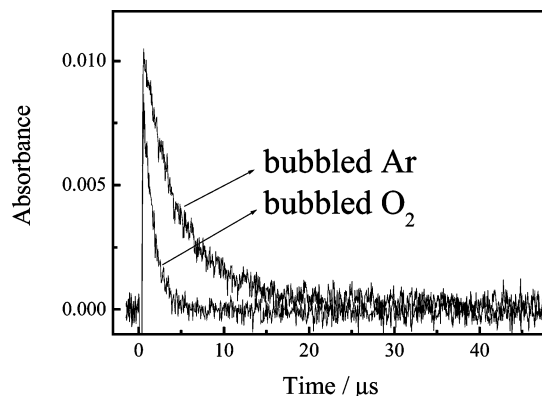


Figure 2. Decay time profiles of $^3\text{NQ}^*$ at 400 nm in Ar-bubbled and O_2 -bubbled acetonitrile.

μs , respectively. High excitation doses will shorten the lifetime of $^3\text{NQ}^*$ due to T–T annihilation.²¹ Relative data of $^3\text{NQ}^*$ were also measured in benzene for comparison.

$$1/\tau = 1/\tau_0 + k_{\text{sq}}[\text{NQ}] \quad (1)$$

Measured τ_0 in benzene (9.77 μs) is a little smaller whereas k_{sq} ($5.50 \times 10^8 \text{ M}^{-1} \text{ s}^{-1}$) is a little larger than the values in acetonitrile.

For $^3\text{NQS}^*$, measured τ_0 and k_{sq} values in acetonitrile were estimated to be $2.84 \times 10^8 \text{ M}^{-1} \text{ s}^{-1}$ and 16.7 μs , respectively. The prolonged lifetime is due to the influence of SO_3Na substituent on the C-4 position of NQS, which will profoundly affect the photophysical and photochemical properties of this molecule.

TABLE 1: Quenching Rate Constants for the Triplets of NQ(NQS) by Different Quenchers in Benzene and Acetonitrile, Oxidation Potentials of Quenchers in Acetonitrile, Free Energy Changes for NQ in Acetonitrile and λ_{\max} of Radical Cations of Quenchers in Acetonitrile

quencher	$k_q/10^9 \text{ M}^{-1} \text{ s}^{-1}$			E_{ox}/V vs SCE ^a	$\Delta G/\text{eV}^a$	λ_{\max} of radical cations/nm ^a
	NQ ^a	NQS ^a	NQ ^b			
DABCO	7.82	9.21	17.4	0.57 ^c	-0.4	450 ^d
DMT	5.74	7.04	16.6	0.7, ^e 0.65 ^f	-0.3, -0.35 ^g	480
TMA	3.69	6.29	13.7	0.74 ^f	-0.26 ^g	510
DMA	2.16	4.84	9.71	0.81, ^h 0.82	-0.2, -0.19 ^g	465 ⁱ
TPA	1.88	2.79	4.72	0.85 ^j	-0.15	360, 550, 650 ^j
DPA	1.79	2.73	3.89	0.84 ^k	-0.16	680 ^j
TEA	0.414	0.637	4.09 (6.8) ^m	0.96 ⁿ	-0.04	<350 ^o
DMABA	0.393	0.582	3.35	1.13 ^f	0.13 ^g	<i>p</i>

^a In acetonitrile. ^b In benzene. ^c Reference 26. ^d Reference 27. ^e Reference 28. ^f Calculated results in this work. ^g ΔG values calculated using E_{ox} values derived from B3LYP methods in this work. ^h Reference 29. ⁱ Reference 30. ^j Reference 31. ^k Reference 32. ^l Reference 33. ^m Reference 21. ⁿ Reference 34. ^o Reference 35. ^p Cannot be found in the range 350–750 nm.

TABLE 2: Quenching Rate Constants ($k_q/\text{M}^{-1}\text{s}^{-1}$) for the Triplets of NQ(NQS) by Different H-Atom Donors in Benzene and Acetonitrile

quencher	NQ ^a	NQ ^b	NQS ^a
cyclohexane	<i>c</i>	4.12×10^5 (4.5×10^5) ^d	<i>c</i>
ethanol	2.34×10^5 (1.6×10^5) ^e	7.58×10^6	2.6×10^5
2-propanol	1.01×10^5 (2.3×10^5) ^e	2.09×10^7	6.82×10^5
benzyl alcohol	1.93×10^6	9.56×10^7	1.06×10^6
sec-butanol	1.06×10^6	5.58×10^7	4.1×10^6
phenethyl alcohol	9.60×10^5	2.26×10^7	1.73×10^6
phenol	1.93×10^8	8.21×10^8	1.56×10^9
1,3-dihydroxybenzene	1.14×10^9	2.49×10^9	1.97×10^9
1,4-dihydroxybenzene	1.58×10^9	2.68×10^9	2.21×10^9

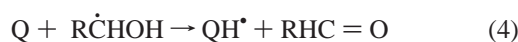
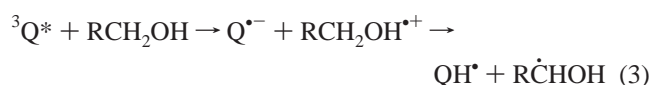
^a In acetonitrile. ^b In benzene. ^c Cannot be obtained accurately. ^d Reference 21. ^e Reference 19.

2. Bimolecular Rate Constants Measurement. In the photoinduced reaction the strongly active nature of quinone triplets makes it easy to abstract an electron or H-atom from different substrates. To unveil the mechanisms of electron/H-atom transfer reactions, laser flash photolysis was carried out with NQ (NQS) and a variety of quenchers in acetonitrile and benzene, respectively. Quenching experiments were chosen at the band of 400 nm for NQ (NQS) to avoid disturbance. Bimolecular quenching rate constants for the reactions of $^3\text{NQ}^*$ ($^3\text{NQS}^*$) with a variety of quenchers are obtained by plotting the observed rate constants (k_{obs}) versus the quenchers' concentration according to

$$k_{\text{obs}} = k_0 + k_q[\text{quencher}] \quad (2)$$

where k_0 and k_q denote the decay rate of triplets in the absence and presence of quencher, respectively. The k_q values including H-atom and electron transfer reactions were determined in polar and nonpolar solvents, as listed in Tables 1 and 2.

3. H-Atom Abstraction. H-atom abstraction by the triplet states of quinones is the most thoroughly studied photochemical reaction.³⁶ Previous works have proved that H-atom abstraction occurs efficiently from 2-propanol and ethanol to $^3\text{NQ}^*$ in either polar or nonpolar solvents.^{19,21} The general H-atom transfer mechanism is depicted as follows:



We repeated the same experiments of NQ with ethanol and 2-propanol and got the similar k_q values. In addition, several other aliphatic and benzylic alcohols were chosen to quench $^3\text{NQ}^*$ ($^3\text{NQS}^*$) in acetonitrile and benzene, obtained values are listed in Table 2.

Phenolic hydrogen abstraction is known to be faster than benzylic and alcoholic hydrogen abstraction.³⁷ This was confirmed in our experiments when H-atom donors were replaced by phenol and diphenols (see Table 2). This large difference comes from the different H-atom abstraction mechanisms, as concluded in previous results.³⁸ In the alcohol/NQ(NQS) system, a direct H-atom abstraction from the aliphatic hydrocarbon takes place. As for the phenol/NQ(NQS) system, the H-atom originating from phenol is a protic H, which is more reactive. Considering the difference, higher quenching rate constants for phenols than for alcohols are understandable. Yoshihara has investigated the H-atom abstraction reactions between 1,4-anthraquinone (AQ) and diverse phenols and proposed that the protic H-atom phenols are ready to be transferred to the triplets of AQ with $^3(\pi, \pi)^*$ character due to the Coulombic interaction in the triplet exciplexes with substantial charge transfer character, resulting in the corresponding semiquinone (AQH \cdot) and phenoxy radicals (RPhO \cdot).³⁷

Cyclohexane is always considered to be a pure H-atom donor. But in our experiment, the decay trace at 400 nm of $^3\text{NQ}^*$ ($^3\text{NQS}^*$) is not quenched distinctly when the concentration of cyclohexane is up to 0.6 M in acetonitrile. When the solvent was replaced by benzene, observable changes are detected ($k_q = 4.12 \times 10^5 \text{ M}^{-1} \text{ s}^{-1}$) from decay curves for NQ/cyclohexane system. This result indicates the higher reactivity of $^3\text{NQ}^*$ in nonpolar solution.

4. Electron Transfer Reactions with Aliphatic Amines. Previously, the photoreduction of various *p*-quinones by DABCO and TEA has been widely investigated and a comprehensive description on the dynamics mechanism was provided by laser flash photolysis studies. In this paper DABCO and TEA were introduced in the experiments with NQ(NQS) in polar and nonpolar solvents. High rate constants for the quenchers were obtained.

The absorption for the TEA radical cation is lower than 350 nm.³⁵ Results from pulse photolysis denoted that the transient absorption band of the NQ radical anion locates at 260 nm with a ϵ (molar extinction coefficient) of $4.0 \times 10^4 \text{ M}^{-1} \text{ cm}^{-1}$, whereas the absorption band of NQ semiquinone radical is smaller than 260 nm with a ϵ of $1.6 \times 10^4 \text{ M}^{-1} \text{ cm}^{-1}$.^{8a} Owing to these reasons, we could not find any newly formed peaks in the range from 350 to 800 nm for the NQ/TEA system except for the obvious quenching at 390 nm for $^3\text{NQ}^*$ by TEA. Generally, products derived from the photolysis involving TEA

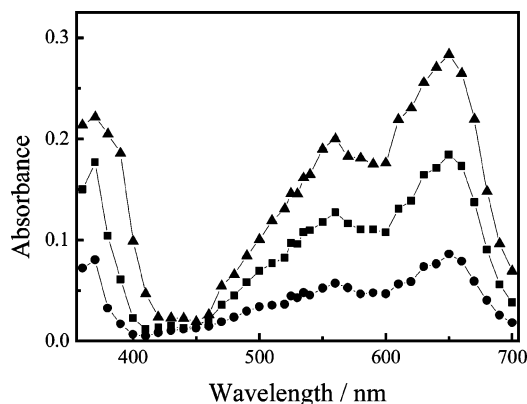


Figure 3. Transient absorption spectra of NQ (0.37 mM) in the presence of TPA (0.18 mM): 700 ns (\blacktriangle), 6 μ s (\blacksquare) and 25 μ s (\bullet) after 355 nm laser pulse in Ar-saturated acetonitrile.

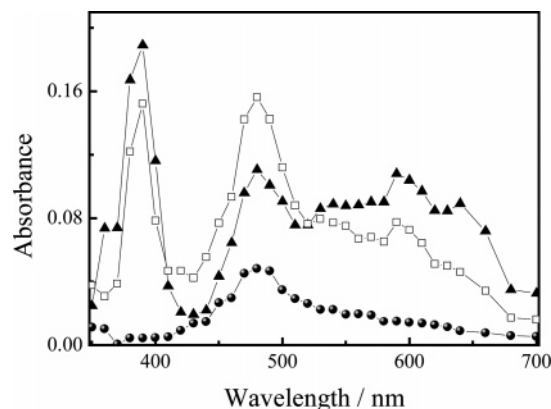


Figure 4. Transient absorption spectra of NQ (0.52 mM) in the presence of DMT (0.077 mM): 600 ns (\blacktriangle), 1.4 μ s (\square) and 40 μ s (\bullet) after 355 nm laser pulse in Ar-saturated acetonitrile.

were more complex than those of primary and secondary amines. A proton transfer process after the initial electron transfer was deduced.¹⁷

Irradiating of NQ and DABCO in degassed acetonitrile led to the formation of a detectable transient at 450 nm (Table 1). This new formed peak is assigned to absorption of the DABCO radical cation, as described previously.²⁷ H-atom transfer is impossible because of its non-hydrogen donating character. The same experiments were repeated on NQS, and similar results with NQ were often obtained.

5. Electron Transfer Experiments with Aromatic Amines.

Evidence for the electron transfer mechanism was obtained from the time-resolved transient spectra of a solution of acetonitrile or benzene containing NQ(NQS) and a series of aromatic amines. On laser flash photolysis of NQ in the presence of TPA, which cannot donate hydrogen, three transient absorption bands located at 360, 550, 650 nm are formed along with the obvious quenching of $^3\text{NQ}^*$ at 400 nm, as shown in Figure 3. These three peaks are assigned to the absorption of the TPA radical cation, which is supported by previous work.³¹ The observations suggest that the reaction pathway involves electron transfer. When the quencher was replaced by secondary amine DPA, the same mechanism was brought out by detecting the distinguishable radical cation of DPA in absorption spectra.

Laser photolysis was also employed on four aniline derivatives with similar configurations. Figure 4 shows the transient spectra obtained from NQ/DMT in Ar-saturated acetonitrile. After the laser pulse, a newly formed peak with the maximum at 480 nm was detected along with the fast decay of $^3\text{NQ}^*$.

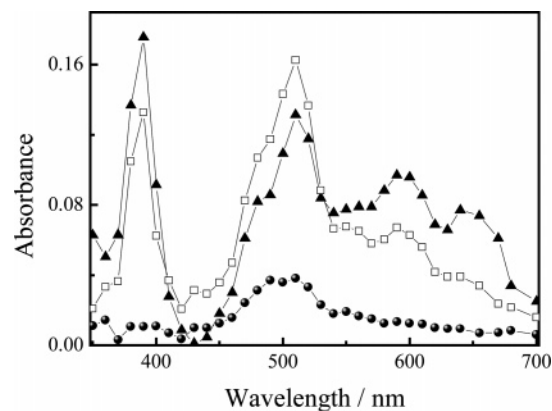


Figure 5. Transient absorption spectra of NQ (0.51 mM) in the presence of TMA (0.14 mM): 600 ns (\blacktriangle), 1.4 μ s (\square) and 40 μ s (\bullet) after 355 nm laser pulse in Ar-saturated acetonitrile.

This long-lived transient at 480 nm is attributed to the radical cation of DMT. Such attribution of the peak at 480 nm was validated by the experiment including 1,4-naphthoquinone (1,4-NQ) and DMT, where the well-characterized absorption peak of the 1,4-NQ radical anion around 390 nm was formed, so the residual located at 480 nm belongs to the radical cation of DMT. Similar behaviors are seen with quenchers TMA and DMA. Two new peaks at 510 and 465 nm in acetonitrile are ascribed to the radical cations of TMA (Figure 5) and DMA,³⁰ respectively. Obviously, electron transfer processes exist in these photoinduced reactions.

Another substituted aniline, DMABA, could quench the absorption at 400 nm of NQ/NQS without any distinct changes in the transient spectra. This is probably due to the low molar coefficient of DMABA radical cation in the range from 350 to 750 nm. Another probable reason may be the formation of partial charge transfer complex rather than electron transfer pathway. Due to the positive free energy change (ΔG_{ct}), such an amine/quinone complex may not undergo rapid dissociation to a radical ion, which could be detected in transient spectra. The triplet states of NQ and NQS are quenched by DMABA with rate constants of 3.93×10^8 and $5.82 \times 10^8 \text{ M}^{-1} \text{ s}^{-1}$, respectively, in acetonitrile, which are clearly smaller than the values for the other three aniline derivatives.

6. Quantum-Chemical Calculation. Fu et al. have successfully employed DFT methods to predict the standard redox potentials of more than 270 kinds of structurally unrelated organic molecules and free radicals in acetonitrile.²⁴ Good correlations were found for the experimental values and calculated values. In this work we use the same method by introducing a solvation model to obtain the unknown redox potentials of several molecules in our experiments. In addition, other useful data such as bond length, bond angle, gas-phase ionization/affinity potentials and charge density distribution for the molecules were also obtained by quantum chemistry calculation.

Figure 6 shows the structures and atomic numberings of two sensitizers. The optimized bond lengths of NQ, $\text{NQ}^{\cdot-}$, NQS and $\text{NQS}^{\cdot-}$ are depicted in Table 3. It seems that C-4 substituted SO_3Na does not affect the geometry of planar naphthoquinone extremely, because neutral and anionic molecular bond lengths for these two quinones are nearly the same. After charge transfer processes, we found that C=O and C₅=C₆ bonds of NQ(NQS) are elongated by 0.03–0.04 and 0.02–0.03 nm, respectively. Such changes indicate that added charge is mostly located on these parts, which are consistent with the changes of calculated charge density distribution of corresponding atoms (not shown).

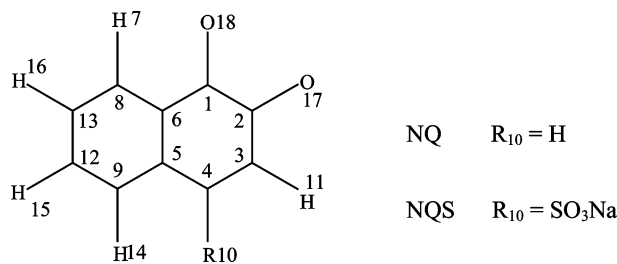


Figure 6. Structures and atomic numberings of NQ and NQS.

TABLE 3: Optimized Geometrical Parameters (Bond Lengths/Å) of NQ, NQS and Their Radical Anions

	NQ	NQ ^{•-}	NQS	NQS ^{•-}
C1–C2	1.562	1.501	1.553	1.470
C2–C3	1.470	1.454	1.469	1.447
C3–C4	1.352	1.374	1.352	1.378
C4–C5	1.464	1.435	1.478	1.446
C5–C6	1.417	1.433	1.421	1.432
C6–C1	1.450	1.477	1.489	1.483
C1–O18	1.218	1.256	1.219	1.250
C2–O17	1.221	1.261	1.221	1.261

TABLE 4: Hammett σ Constants, Calculated Ionization Potentials, Change Density on N-Atom and Oxidation Potentials of Anilines in the Gas Phase/Acetonitrile

substrate	IP/eV	E_{ox}/V vs SCE (in acetonitrile)	Hammett σ constant	charge density (N-atom)	
				neutral	cation
DMT	6.81	0.65	-0.17	-0.175	0.11
TMA	6.80	0.74	-0.14	-0.182	0.12
DMA	7.05	0.82	0	-0.07	0.036
DMABA	7.38	1.13	0.45	0.039	-0.089

DFT-B3LYP methods were used to predict the electron affinities and reduction potentials of NQ and NQS, because MP2 and molecular orbital based HF methods are not accurate enough to do so.^{39,40} Electron affinity (EA) of NQ is 2.13 eV. SO₃Na at the C-4 position reduces the EA value to 2.08 eV. The calculated E_{red} of NQS (-0.49 V) is a little more positive than that of NQ (-0.58 V), which means the stronger oxidation property for NQS.

The gas-phase ionization potentials (IP), charge density on N-atom of anilines and oxidation potentials in acetonitrile were also calculated, and the results are listed in Table 4. Because these four aniline derivatives have similar molecular structural conformations, it would be helpful to get information from ab initio calculation to interpret the reactivities of anilines in the quenching reactions. Optimized geometries of these anilines are shown in Figure 7. The charge densities on the N-atom of these neutral anilines are negative except for DMABA. Due to the electron-abstracting nature of substituted COOH, DMABA has a positive value. In our calculation the values of IP and charge densities were obtained in the gas phase, but E_{ox} was obtained in solution. It is notable that in Table 4 the trend of E_{ox} values calculated for DMT and TMA is a little different from the trend of IP and charge densities gained from the gas phase. Due to the impact of solvation free energy in acetonitrile, DMT has the smallest E_{ox} , which is in accordance with the authentic experimental k_q and ΔG values.

Discussion

Quenching rate constants of H-atom transfer for five alcohols and three phenols with NQ/NQS were investigated. Compared with the k_q values for ethanol and 2-propanol, three other alcohols have obviously larger rate constants in acetonitrile and

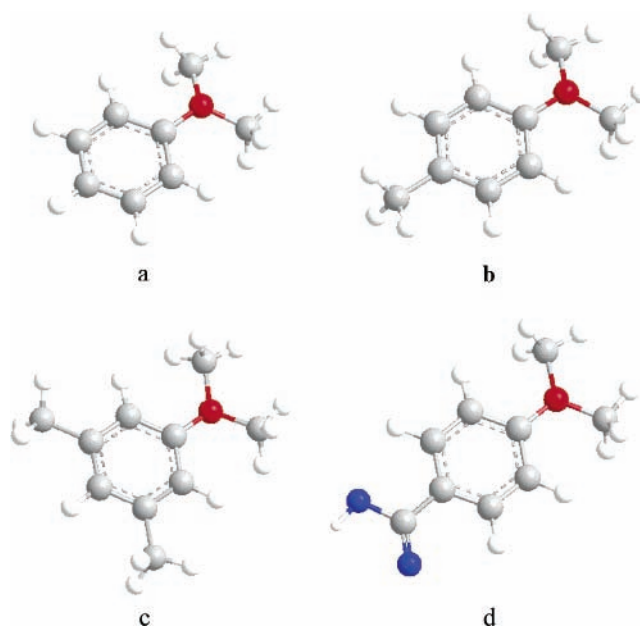


Figure 7. Geometries of (a) DMA, (b) DMT, (c) TMA and (d) DMABA in the ground states.

benzene, as shown in Table 2. It seems that the benzenoid structure and long aliphatic chain possibly increase H-donating abilities of various alcohols. As for three phenols, we found a smaller k_q for phenol compared with diphenols (1,3-dihydroxybenzene and 1,4-dihydroxybenzene) in the reactions with NQ and NQS. This is understandable because diphenol has one extra hydroxy group compared to phenol.

Barra et al. have pointed out the reactivity of *o*-quinone triplets is higher in benzene solution as compared with that in acetonitrile solution.²¹ This conclusion is true in our quenching experiments. In H-atom abstraction reactions, especially for 2-propanal and phenethyl alcohol, quenching rate constants in benzene reach $10^7 \text{ M}^{-1} \text{ s}^{-1}$, which are 2 orders of magnitude greater than the rate constants obtained in acetonitrile. Analogously, all the quenching rate constants measured in benzene are actually 2–10 times higher than those measured in acetonitrile, as shown in Table 1. The increased reactivity in benzene can be explained by a conversion of excited-state configuration of NQ(S) from ${}^3(\pi, \pi)^*$ to ${}^3(n, \pi)^*$,^{20,21} as described before.

Another important experimental conclusion is related to the different trends of quenching rate constants for NQ and NQS; i.e., observed k_q values for NQS are obviously larger than those for NQ. This is the direct result of the different excited-state configurations for two sensitizer molecules. Due to the impact of a covalent electron-releasing group SO₃Na on the C-4 position of the phenyl ring, electron cloud densities on oxygen atoms of NQS are much rarer. So compared with NQ, NQS is more propitious to abstract an electron from various donors. Clearly, it could be deduced that the excited-state reduction potential E_{red}^* of NQS should be higher than that of NQ, and this assumption has been proved by quantum chemistry calculation.

Especially, it is very interesting that the experimental k_q values obtained in polar or nonpolar solvent for four anilines increase in the order DMABA < DMA < TMA < DMT, for both NQ and NQS. As electron transfer reactions take place from the charge-centralized “N” atoms of aniline molecules, it is easy to understand the k_q values are in accordance with the charge densities of “N” atoms. This phenomenon can be validated by either of the following: (i) good correlation between Hammett constants σ and $\log k_q$ or (ii) good correlation between E_{ox} values and $\log k_q$.

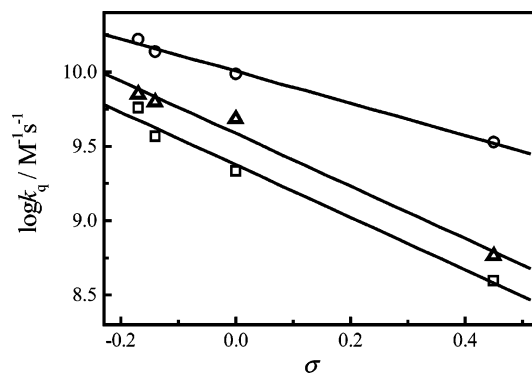


Figure 8. Linear dependence of $\log k_q$ for the anilines on the σ values of different substituents: (○) NQ in benzene, (△) NQS in acetonitrile, (□) NQ in acetonitrile.

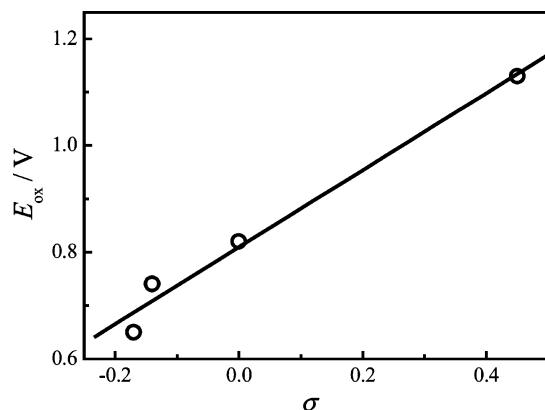


Figure 9. Linear dependence of E_{ox} values on the Hammett σ constants.

(i) From Figure 8, we can observe that $\log k_q$ values obtained from reactions are in good correlation with the Hammett σ constants.⁴¹ It means the higher electron-donating ability of the substituent will increase the charge density on the “N” atom and accelerate the proposed electron transfer reaction. Negative ρ values of -1.77 for NQ in acetonitrile (-1.08 in benzene) and -1.77 for NQS in acetonitrile were obtained from the slopes. These negative values suggest the electrophilic nature of carbonyl triplets.⁴²

(ii) The E_{ox} values and charge densities on the N atom for these neutral anilines were calculated by the DFT method. Considering the solvation free energy, the calculated oxidation potentials for the four anilines in acetonitrile decrease in the order DMABA (1.13 V) > DMA (0.82 V) > TMA (0.74 V) > DMT (0.65 V). Generally, small E_{ox} means strong electron-donating ability. So DMT should have the largest k_q value and DMABA should have the smallest one. We can easily find this trend in Table 1.

In addition, from the preceding two aspects we found the good correlation between Hammett σ constants and E_{ox} values obtained from quantum calculation, as shown in Figure 9. This is useful to evaluate the corrections of both kinds of values from diverse research realms.

We have proposed the existence of electron transfer interactions between NQ(NQS) and amines from laser photolysis experiments. To further approve the thermodynamic feasibility, we try to determine the rate constants in quenching reactions as a function of the free energy change ΔG , which could be calculated by

$$\Delta G = E_{\text{ox}} - E_{\text{red}} - q^2/\epsilon r - E_T \quad (6)$$

where E_{ox} (in V) and E_{red} (in V) are the oxidation potential of

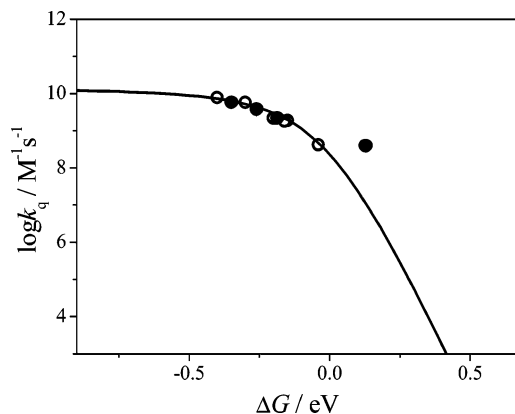


Figure 10. Rehm–Weller correlation plot of $\log k_q$ vs ΔG for NQ and amines/anilines: (○) ΔG calculated by using experimental E_{ox} values, (●) ΔG calculated by using E_{ox} values derived from B3LYP method.

the donor and the reduction potential of the acceptor, respectively. E_T (in eV) is the excited-state energy of the sensitizer. For NQ, the value of E_{red} is -0.58 V (vs SCE) in acetonitrile.²⁸ $q^2/\epsilon r$ is the work term that accounts for the Coulombic energy of the product ions at the encounter distance ($q^2/\epsilon r = 0.055$ eV in acetonitrile). E_T has been estimated to be around 35 kcal/mol by theoretical calculation,²⁵ which is close to the value derived from our triplet sensitization experiment. The plot of $\log k_q$ vs ΔG shown in Figure 10 correlates well with the solid line derived from the Rehm–Weller relationship⁴³ and exhibits a typical feature of the photoinduced electron transfer process. Most of the experimental k_q values are approximate to the calculated ones except for that of DMABA with a positive ΔG value, as depicted in Table 1. This slight deviation may be the result of existence of an exciplex-formation process.^{44,45}

Conclusions

The photoinduced reactions of the excited NQ (NQS) with H-atom/electron donors were studied by laser flash photolysis. Compared with NQ, NQS was found to be more active to react with all the quenchers in terms of configuration analysis. This suggestion is in good agreement with the quenching rate constants obtained from flash photolysis; i.e., k_q values for NQS are all larger than values of NQ. The solvent effect is obvious for NQ in acetonitrile and benzene. This phenomenon is the direct result of the special excited-state configuration for NQ. To further confirm the reaction mechanism, laser flash photolysis was introduced to gain the time-resolved absorption spectra. The electron transfer pathway was thought to happen along with the evidence from thermodynamic data. Furthermore, k_q values for the four aniline derivatives with NQ(NQS) in solution were discussed according to the Hammett equation. Substituent effects dominate the reactivities of various anilines.

Acknowledgment. This research is supported by the National Natural Science Foundation of China (No. 20273066).

References and Notes

- Burie, J.-R.; Boussac, A.; Boullais, C.; Berger, G.; Mattioli, T.; Mioskowski, C.; Nabedryk, E.; Breton, J. *J. Phys. Chem.* **1995**, *99*, 4059–4070.
- Patai, S., Ed. *The Chemistry of the Quinoid Compounds*; Wiley: New York, 1974.
- Plalniappan, V.; Martin, P. C.; Chynwat, V.; Frank, H. A.; Bocian, D. F. *J. Am. Chem. Soc.* **1993**, *115*, 12035.
- Kirmaier, C.; Holten, D. *Photosynthesis Res.* **1987**, *13*, 260.
- Robinson, H. H.; Crofts, A. R. *FEBS Lett.* **1983**, *153*, 221–226.

- (6) Loeff, I.; Rabani, J.; Treinin, A.; Linschitz, H. *J. Am. Chem. Soc.* **1993**, *115*, 8933.
- (7) Loeff, I.; Treinin, A.; Linschitz, H. *J. Phys. Chem.* **1984**, *88*, 4931.
- (8) (a) Rao, P. S.; Hayon, E. *J. Phys. Chem.* **1973**, *77*, 2274 (b) Brahmia, O.; Richard, C. *Photochem. Photobiol. Sci.* **2003**, *2*, 1038 (c) GöFrner, H. *Photochem. Photobiol.* **2005**, *81*, 367.
- (9) Eggins, B. R.; Robertson, P. K. *J. Chem. Soc., Faraday Trans.* **1994**, *90*, 2249.
- (10) Balakrishnan, G.; Mohandas, P.; Umapahty, S. *J. Phys. Chem.* **1996**, *100*, 16472.
- (11) Grafton, A. K.; Wheeler, R. A. *J. Phys. Chem. A* **1997**, *101*, 7154.
- (12) Wang, S. K. *J. Am. Chem. Soc.* **1978**, *100*, 5488.
- (13) Loeff, I.; Goldstein, S.; Treinin, A. *J. Phys. Chem.* **1991**, *95*, 4423.
- (14) Treinin, A.; Hayon, E. *J. Am. Chem. Soc.* **1976**, *98*, 3884.
- (15) Yamaji, M.; Kurumi, M.; Kimura, H.; Shizuka, H. *Phys. Chem. Chem. Phys.* **1999**, *1*, 1859.
- (16) Scheerer, R.; Grätzel, M. *J. Am. Chem. Soc.* **1977**, *99*, 865.
- (17) Ci, X. H.; Silva, R. S.; Nicodem, D.; Whitten, D. G. *J. Am. Chem. Soc.* **1989**, *111*, 1337.
- (18) Silva, R. S.; Nicodem, D. E. *J. Photochem. Photobiol. A* **2004**, *162*, 231.
- (19) Harada, Y.; Watanabe, S.; Suzuki, T.; Ichimura, T. *J. Photochem. Photobiol. A* **2005**, *170*, 161.
- (20) Shimoishi, H.; Tero-Kubota, S.; Akiyama, K.; Ikegami, Y. *J. Phys. Chem.* **1989**, *93*, 5410.
- (21) Barra, M.; Harder, E. D.; Balfe, J. P. *J. Chem. Soc., Perkin Trans. 2* **1999**, 1439.
- (22) Pan, Y.; Zhao, J. S.; Ji, Y. Y.; Yan, L.; Yu, S. Q. *Chem. Phys.* **2006**, *320*, 125.
- (23) Pan, Y.; Sheng, Z. Y.; Ye, X. D.; Ao, Z.; Yu, S. Q. *J. Photochem. Photobiol. A* **2005**, *174*, 98.
- (24) Fu, Y.; Liu, L.; Yu, H. Z.; Wang, Y. M.; Guo, Q. X. *J. Am. Chem. Soc.* **2005**, *127*, 7227.
- (25) Becker, R. S.; Natarajan, L. V. *J. Phys. Chem.*, **1993**, *97*, 344.
- (26) Nelsen, S. F.; Hinz, P. J. *J. Am. Chem. Soc.* **1972**, *94*, 7114.
- (27) Fukuzumi, S.; Ohkubo, K.; Suenobu, T.; Kato, K.; Fujitsuka, M.; Ito, O. *J. Am. Chem. Soc.* **2001**, *123*, 8459.
- (28) Meites, L.; Zuman, P. *CRC Handbook Series in Organic Electrochemistry*; CRC Press Inc.: Boca Raton, FL, 1976; Vol. 1.
- (29) Nocera, D. G.; Gray, H. B. *J. Am. Chem. Soc.* **1981**, *103*, 7349.
- (30) Shida, T.; Nosaka, Y.; Kato, T. *J. Phys. Chem.* **1978**, *82*, 2, 695.
- (31) Bartholomew, R. F.; Davidson, R. S.; Lambeth, P. F.; Mckellar, J. F.; Turner, P. H. *J. Chem. Soc., Perkin Trans.* **1972**, *2*, 577.
- (32) Dvorak, V.; Nemeč, I.; Zyka, J. *J. Microchem. J.* **1967**, *12*, 99.
- (33) Shida, T.; Hamill, W. H. *J. Chem. Phys.* **1966**, *44*, 2369.
- (34) Fichter, F. *Organische Elektrochemie*; Steinkopff: Dresden, 1942; pp 124.
- (35) Amada, I.; Yamaji, M.; Tsunoda, S.; Shizuka, H. *J. Photochem. Photobiol. A*: **1996**, *95*, 27.
- (36) Wagner, P.; Park, B.-S. *Org. Photochem. II* **1991**, 227.
- (37) Yoshihara, T.; Yamaji, M.; Itoh, T.; Shizuka, H.; Shimokage, T.; Tero-Kubota, S. *Phys. Chem. Chem. Phys.* **2000**, *2*, 993.
- (38) Lucas, N. C.; Netto-Ferreira, J. C. *J. Photochem. Photobiol. A* **1998**, *116*, 203.
- (39) Almlöf, J. E.; Feyereisen, M. W.; Jozefiak, T. H.; Miller, L. L. *J. Am. Chem. Soc.* **1990**, *112*, 1206.
- (40) Jursic, B. S. *J. Mol. Struct. (THEOCHEM)* **1998**, *452*, 145.
- (41) Johnson, C. D. *The Hammett Equation*; Cambridge University Press: Cambridge, U.K., 1973.
- (42) Das, P. K.; Bhattacharyya, S. N. *J. Phys. Chem.* **1981**, *85*, 1391.
- (43) Rehm, D.; Weller, A. *Isr. J. Chem.* **1970**, *5*, 259.
- (44) Pal, H.; Palit, D. K.; Mukherjee, T.; Mittal, J. P. *J. Chem. Soc., Faraday Trans.* **1993**, *89*, 683.
- (45) Kuzmin, M. G. *Pure Appl. Chem.* **1993**, *65*, 1653.